Optimization-based Online Decision Support Tool for Electric Arc Furnace Operation[⋆]

Smriti Shyamal [∗] **Christopher L.E. Swartz** [∗]

[∗] *Department of Chemical Engineering, McMaster University,*
1280 Main St W, Hamilton ON L8S 4L7, Canada
(e-mail: swartzc@mcmaster.ca).

Abstract: Electric arc furnaces (EAFs) are broadly used in the steel industry for producing different grades of steel by melting steel scrap and modifying its chemistry. The EAF process is highly energy intensive and involves a low level of automation. The decisions associated with the amount and timing of injected inputs depend heavily on the EAF operators. Although the operators' practical experience is crucial in running the EAF, important multivariable interactions and subtle relationships may not be apparent. In this work, a multi-rate moving horizon estimator (MHE) is coupled with an economics-based dynamic optimizer to form an online decision support tool (DST). The tool is able to reconstruct the states and provide optimal decisions to operators in less than 18 CPU seconds on average despite the use of a highly nonlinear large-scale EAF model. This framework is developed using entirely open source tools to have a high appeal to industrial practitioners. A case study is presented which demonstrates the increase in profit through the use of the DST.

Keywords: Moving horizon estimation, dynamic optimization, electric arc furnace, multi-rate measurements, decision support tool, on-line optimization.

1. INTRODUCTION

Electric arc furnaces (EAFs) are being successfully used in the steelmaking industry for recycling scrap by melting it down and altering its chemistry to achieve the desired product grade. Melting of steel is a highly energy intensive complex batch process involving both electrical and chemical energy. Multiple electrodes are used to transfer electrical power to the furnace while natural gas and oxygen injected through burners provide the chemical energy post-combustion. A pool of molten steel is formed at the base of the arc as the batch (heat) progresses. A slag layer is formed on top of the pool due to oxygen reacting with the metal to form oxides. Slag chemistry is adjusted by direct addition of carbon, dolomite, and lime through the furnace roof and by appropriate oxygen and carbon lancing. The high energy intensive nature of the process motivates the development of advanced estimation and control strategies for an industrial EAF.

EAFs are typically operated with a low level of automation and a lot of operator involvement. Although the experience-based knowledge of operators is useful for the EAF operation, this understanding can be limited due to the multivariable nature of the complex process and underlying relationships which may be overlooked. Subsequently, process operating procedures are based upon what has worked well in the past in most situations. Research efforts have been directed towards developing a detailed dynamic mathematical model to describe the melting process, chemical changes and account for reagent and energy additions. The model can then be used within a mathematical optimization procedure to determine the optimal trajectories for the process inputs. However, a characteristic of this process that makes the online application of optimization more complex, is the small number of online process measurements from which it is difficult to infer the current state of the process. Billings et al. (1979) applied the extended Kalman filter (EKF) to reconstruct the states for the refining stage of EAF operation but the application model contained 4 states, which is too few to capture the detailed process dynamics. Ghobara (2013) implemented a multi-rate version of EKF to handle varying sampling rates of the measurements taken during a typical heat.

Of the many reported tools for state estimation, moving horizon estimation (MHE) has become quite popular (Allgöwer et al., 1999) due to its constraint handling ability and the use of computationally efficient numerical optimization algorithms. MHE involves solving a nonlinear dynamic optimization problem subject to the nonlinear system under consideration and other relevant constraints. The use of a finite set of past available measurements by MHE to reconstruct the full state vector keeps the optimization problem numerically tractable. Although for batch processes, an expanding horizon for MHE would reduce the loss of information, it would increase the on-line computational burden, potentially leading to delayed feedback action. The finite size window of measurements also provides a natural framework to include measurements with different sampling rates. Shyamal and Swartz (2016b)

demonstrated a parameter estimation based multi-rate MHE strategy for a short simulation horizon of an EAF heat. The MHE application was then implemented for the entire duration of the EAF batch by Shyamal and Swartz (2016a).

In this article, we extend the results of Shyamal and Swartz (2016a) by developing an online decision support tool (DST) which uses the multi-rate MHE to provide the state knowledge to an economics-based optimizer for improved performance. Objectives other than economics have also been reported in the literature, such as minimizing power (Woodside et al., 1970), model predictive control's (MPC) set-point tracking objective function (Oosthuizen et al., 1999) to determine optimal inputs, and a weighted function to minimize the offgas CO content, the final FeO and the final time (Matson and Ramirez, 1999). MacRosty and Swartz (2007) showed that a dynamic optimization procedure can effectively maximize the profit while considering the trade-offs between the process inputs and processing time. To solve the optimization problem, they employed a sequential approach which can be time-consuming particularly when repeated optimizations needs to be carried out involving a large-scale differential-algebraic equation (DAE) model (Biegler, 2007). On the other hand, the simultaneous approach for dynamic optimization can become quite useful for real time applications such as an online DST. The simultaneous approach using implicit Euler discretization is employed in this work for both the estimator and the shrinking horizon optimizer to achieve a reasonable CPU solve. The first-principles based dynamic model developed in MacRosty and Swartz (2005) is utilized to develop the online DST for the EAF operators. The DST framework involves the state estimator running in parallel with the plant while the shrinking horizon optimizer can be called multiple times during the batch duration as desired by the operators. The potential economic improvement achieved though the use of the DST is illustrated through application to a case study.

2. EAF MODEL OVERVIEW

The EAF model developed by MacRosty and Swartz (2005) considered 4 zones for the furnace:

(1) the *gas zone* includes all gases present in the free space of furnace above the scrap material;
(2) the *slag-metal interaction zone* contains all the slag material and the part of molten steel zone in contact with it;
(3) the *molten steel zone* comprises the metals in their liquid state after the scrap has melted, excluding the part included in the slag-metal interaction zone;
(4) the *solid scrap zone* consists of remaining solid from the charged scrap.

The first-principles dynamic model is based on equations describing mass and energy balances, chemical equilibrium, and heat transfer relationships. Due to high operating temperatures in the furnace, chemical equilibrium is assumed for the slag-metal and gas zones, and calculated by minimizing the Gibbs-free energy. The reactions are limited by mass transfer between the zones. Figure 1 is a schematic diagram of the process showing inputs, outputs and material flow between the four zones. The
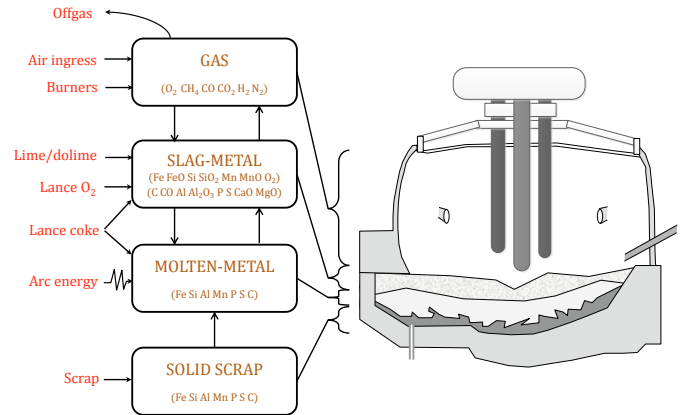

Fig. 1. Schematic of EAF model. (MacRosty and Swartz, 2005)

heat received by the roof and the walls of furnace due to radiation and convection is also modeled. The model considers slag foaming caused by evolution of CO from the molten metal. Estimation of model parameters was carried out using industrial data and validated against additional data not used in the estimation. The original model was modified and reconfigured by Ghobara (2013). Two major changes were applied: first, a flat surface geometry for scrap melting was utilized, unlike cone-frustum assumed by MacRosty and Swartz (2005), and second, three JetBoxes which control the supply of oxygen to the furnace were added. The DAE system was modeled in the commercial software `gPROMS` (Process Systems Enterprise Ltd., 2015) and contained 40 differential variables.

Shyamal and Swartz (2016b) removed the radiation model considered by Ghobara (2013), and replaced it with a new parameter that divides the energy lost from the arc power through radiation between the roof, the walls, the scrap and the molten metal. The model parameters were re-estimated for the modified model, and matching profiles between the plant and model were obtained. They further assumed that all the oxides are present in the slag-metal zone, with the corresponding states removed from the molten metal, except oxygen which is usually required if lancing occurs. The modified EAF model was also coded in `gPROMS` and had 29 states. Shyamal and Swartz (2016a) translated the model to an open-source `Python` framework `CasADi` (Andersson, 2013), which initially contained 28 states and 518 algebraic variables. As the 29th state in the prior model took values which were very small (close to 1.0×10^{-13}), it was removed from the model and replaced with a constant small number. `CasADi` was then employed to eliminate a subset of the algebraic variables and equations by transforming them into dependent variables defined by explicit expressions containing only the differential and algebraic variables. The model reduction exercise, which removed a significant amount of complexity, reduced the variable count to 28 states and 121 algebraic variables. We are using the same model of Shyamal and Swartz (2016a) to carry out the case study presented in the last section of this article.
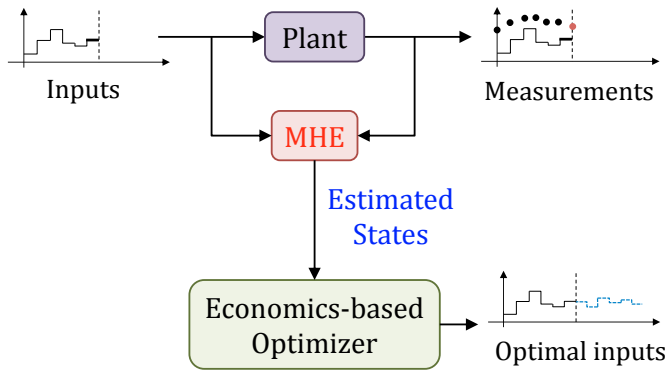
Fig. 2. Online decision support tool for EAF operation

3. DYNAMIC OPTIMIZATION AND MHE BASED ON-LINE DECISION SUPPORT TOOL

In this section, we describe the proposed on-line DST for EAF operation. A key feature of the DST involves a real-time dynamic optimization implementation wherein the model runs in parallel with the plant as shown in figure 2. The model states at any point in the heat reflect the actual plant inputs up to that point. The state variables are inferred on the basis of plant measurements using state estimation. The reason for using a state estimator is to ensure that the unknown initial conditions and disturbances during the batch operation are handled by the model in real-time. Once the state estimates are obtained from MHE, they are sent to a shrinking horizon optimizer which calculates an economically optimal sequence of control variables. The EAF operators can execute the optimizer during the heat whenever they need a recommendation with regard to the optimal input. However, the MHE will automatically be running every 1 minute to calculate the state estimates by minimizing the differences between model predictions and measurements. Furthermore, the operators will access only the final computed optimal inputs, with the other internals of the DST hidden from them.

The optimization procedure in the DST is computationally challenging because real-time solutions of the dynamic optimization problems are needed to avoid delays in passing decision support to the operators. Faster running of the models is achieved though the use of a full discretization approach to solve the infinite dimensional problems. The approach converts the problem into a general nonlinear program (NLP) in purely algebraic form. Quick solutions of the NLP problems are obtained by initializing both the primal and dual variables and using an interior-point solver. The details of formulation and solution strategy are presented in the subsequent subsections.

3.1 Shrinking Horizon Dynamic Optimization

The EAF dynamic optimization problem considered here maximizes the profit per batch, in dollars. Based on the state estimates received from the multi-rate MHE (discussed in next subsection), a shrinking horizon problem with t_f as the fixed final duration of the heat, is formulated. The DAE model equations $\mathbf{h}(\cdot)$ appear in a discretized form as equality constraints. At the current

time t_i, the optimization problem under consideration is given by,

$$\max_{u(t)} \quad c_0 M_{steel}(t_f) - \left(c_1 \int_{t_i}^{t_f} P\,dt + c_2 \int_{t_i}^{t_f} F_{CH_4,brnr}\,dt \right.$$
$$\left. + c_3 \int_{t_i}^{t_f} (F_{O_2,Jetbox1} + F_{O_2,Jetbox2} + F_{O_2,Jetbox3})\,dt \right) \tag{1}$$

subject to
Model equations:
$$\mathbf{0} = \mathbf{h}(\dot{\mathbf{x}}(t), \mathbf{x}(t), \mathbf{u}(t), \mathbf{y}(t), t) \tag{2}$$
Input constraints:
$$P^{min}(t) \leq P \leq P^{max}(t) \tag{3}$$
$$F_k^{min}(t) \leq F_k \leq F_k^{max}(t) \tag{4}$$

where P is the electrical arc power, $F_{CH_4,brnr}$ is the flow rate of natural gas from the burner, and $F_{O_2,Jetbox1}$, $F_{O_2,Jetbox2}$ and $F_{O_2,Jetbox3}$ are oxygen flow rates from Jetboxes 1,2, and 3 respectively. M_{steel} is the mass of liquid steel at the end of the batch and c_k ($k = 0, 1, 2, 3$) is the associated unit cost of each component. The decision variables $u(t)$ for the optimization problem , consisting of P, $F_{CH_4,brnr}$, $F_{O_2,Jetbox1}$, $F_{O_2,Jetbox2}$, and $F_{O_2,Jetbox3}$, are taken as piecewise constants. $\mathbf{x}$ and $\mathbf{y}$ are the differential and algebraic variables of the process model respectively. The four flow rates are represented as F_k in concise form. The input constraints bound the control variables between upper (P^{max}, F_k^{max}) and lower bounds (P^{min}, F_k^{min}) to ensure that the power addition and the flows are allowed to move within realistic bounds. The optimal sequence of the inputs calculated from the above problem provides the decision support to the operators.

3.2 Multi-rate MHE

EAF process operation is significantly complex, and subject to fluctuations due to frequent material additions to the furnace. As a first principles model constitutes an approximation to reality, plant-model mismatch and modeling errors are inevitably present. There are some unknown disturbances as well during the batch operation. The estimation strategy introduced here uses process noise terms to account for uncertainties. Further issues that need to be addressed are the limited availability of measurements, and their availability at different rates. The multi-rate MHE formulation is adopted here to take advantage of both fast and slow measurements.

Consider as a reference point time instant t_i, where i is the current sampling index and a past sequence of inputs and measurements is available. The multi-rate MHE formulation includes measurements with multiple sampling rates. The infrequent measurements related to the molten metal and slag zones are simply introduced in their appropriate locations in the moving horizon window of length N time intervals. Assuming the slow measurements are placed at sampling times corresponding to fast measurements, the vector of only fast measurements is defined as $\mathbf{y}_k^F$ and the vector containing both the slow and fast measurements is defined as $\mathbf{y}_k^{SF}$. The measurement distribution in a moving window can be given as, for example, $\mathbf{Y}_i = \{\mathbf{y}_{i-N}^F, \mathbf{y}_{i-N+1}^{SF}, \mathbf{y}_{i-N+2}^F, \ldots, \mathbf{y}_i^F\}$, where the measurement set at time t_{i-N+1} contains both the slow

and fast measurements. The example can be adapted for different structures of $\mathbf{Y}_i$. At the next sampling time, when a new measurement arrives it is included in the horizon window, and the oldest measurement is dropped.

The multi-rate MHE problem for a nonlinear system which is observable along the state trajectories takes the following general form:

$$\min_{\mathbf{x}_{i-N},\mathbf{w}_k} \sum_{k=i-N}^{i-1} ||\mathbf{w}_k||^2_{Q^{-1}} + \sum_{\substack{k=i-N \\ k \in I_F}}^{i} ||\mathbf{v}_k^F||^2_{(R^F)^{-1}}$$

$$+ \sum_{\substack{k=i-N \\ k \in I_{SF}}}^{i} ||\mathbf{v}_k^{SF}||^2_{(R^{SF})^{-1}} + ||\mathbf{x}_{i-N} - \hat{\mathbf{x}}_{i-N}||^2_{S_i^{-1}}$$

$$(5)$$

$$\text{s.t. } \mathbf{x}_{k+1} = \mathbf{f}(\mathbf{x}_k, \mathbf{u}_k) + \mathbf{w}_k, k = i - N, \ldots, i - 1 \quad (6)$$

$$\mathbf{y}_k^F = \mathbf{h}^F(\mathbf{x}_k) + \mathbf{v}_k^F, \quad k \in I_F \quad (7)$$

$$\mathbf{y}_k^{SF} = \mathbf{h}^{SF}(\mathbf{x}_k) + \mathbf{v}_k^{SF}, \quad k \in I_{SF} \quad (8)$$

$$\mathbf{x}^{LB} \le \mathbf{x_k} \le \mathbf{x}^{UB}, \quad (9)$$

where $\mathbf{w}_k$ is a piecewise constant noise term introduced to model the process noise (i.e. the model uncertainty), $\hat{\mathbf{x}}_{i-N}$ is an estimate for the state at the beginning of the horizon, $\mathbf{f}$ integrates the model, given the system state vector $\mathbf{x}_k$, the control input $\mathbf{u}_k$ and the process noise $\mathbf{w}_k$, over one sampling interval, and $\{\mathbf{h}^F, \mathbf{h}^{SF}\}$ are the measurement functions that map the system state to $\mathbf{y}_k^F$ and $\mathbf{y}_k^{SF}$ respectively. $\mathbf{v}_k^F$ and $\mathbf{v}_k^{SF}$ are the measurement noise terms. The implicit Euler method is employed to generate the discretized form of model (6) from the DAE model. Q, R^F, R^{SF} and S_i are the covariance matrices (of appropriate dimensions) for the model noise, measurement noise and for the arrival cost respectively. $\mathbf{x}^{LB}$ and $\mathbf{x}^{UB}$ represent lower and upper bounds respectively on the state variables.

The cost function (5) contains four terms of which the first three are weighted minimization of errors over a time horizon N. The fourth term of (5), the arrival cost, summarizes the previous measurement data not considered in the moving horizon window. The weighing matrix S_i is updated to S_{i+1} for the next MHE run using the solution of the currently solved MHE optimization problem. An EKF update is generally used (Rao et al., 2003),

$$S_{i+1} = Q + A_i[S_i - S_i C_i^T (R + C_i S_i C_i^T)^{-1} C_i S_i] A_i^{-1}$$

$$(10)$$

where $A_i = \nabla_{\mathbf{x}} \mathbf{f}(\mathbf{x}_{i-N}^*, \mathbf{u}_{i-N}, \mathbf{w}_{i-N}^*)$ and $C_i = \nabla_{\mathbf{y}} \mathbf{h}(\mathbf{x}_{i-N}^*)$. $\mathbf{x}_{i-N}^*$ and $\mathbf{w}_{i-N}^*$ are solution vectors of the MHE optimization problem (5). It is to be noted that for time step $t_i \le N$, a constant initial state covariance matrix is used, and the past window of measurements is allowed to grow without dropping any measurements.

3.3 DST Implementation

The DST is implemented for a discretized model in CasADi using the Python interface. For time discretization we choose 7 and 4 finite elements per time step (1 minute for our case), with the backward Euler scheme, for the multi-rate MHE and the shrinking horizon dynamic optimization respectively. IPOPT (Wächter and Biegler,

Table 1. Result comparison for the case study.

	Theoretical	Nominal	Using DST
Profit [\$/batch]	100	95.39	97.67

2006) using the linear solver MA27 is employed to solve the sparse NLP problem thus obtained. The optimal sequence of inputs computed by the DST is applied to the plant model to get measurements until the shrinking horizon optimizer is called again. Plant and model simulations, required for measurement generation and forward integration, are performed with IDAS (part of the SUNDIALS (Hindmarsh et al., 2005) suite of solvers). To find a good starting point to solve the MHE and the shrinking horizon optimization problem, the primal and the dual variable values are extracted from the respective previous optimization solves. The set of values is truncated by dropping the first time interval values in the case of MHE. A forward simulation is also carried out to obtain an initial guess for the MHE primal variables associated with the new terminal interval. For the shrinking horizon optimizer, appropriate number of the values are removed for time intervals starting from the first one.

The implementation involves a plant-model mismatch created by decreasing a power factor parameter k_p by 10% in the model. This mismatch significantly decreases the amount of energy delivered to the scrap charge due to the arc power input. The model equations where k_p appears can be found in Ghobara (2013). The impact of unmeasured disturbances on the model due to the mismatch is mitigated by augmenting the system state with an integrated disturbance $\mathbf{d}_k$, driven by white noise $\mathbf{w}_{dk}$. We implement the state estimator using the augmented system model

$$\mathbf{x}_{k+1} = \mathbf{f}(\mathbf{x}_k, \mathbf{u}_k) + \mathbf{B}_d \mathbf{d}_k + \mathbf{w}_k \quad (11)$$

$$\mathbf{y}_k = \mathbf{h}(\mathbf{x}_k) + \mathbf{v}_k$$

$$\mathbf{d}_{k+1} = \mathbf{d}_k + \mathbf{w}_{dk}, \quad \mathbf{w}_{dk} \sim \mathcal{N}(0, \mathbf{Q}_d)$$

where $\mathbf{B}_d$ is used to adjust the effect of disturbance state on the system and $\mathbf{Q}_d$ is the covariance of $\mathbf{w}_{dk}$. For the case study conducted, the disturbance state is implemented on the state variable representing moles of manganese in the slag zone model.

4. CASE STUDY

In this section, a case study is presented to demonstrate the economic benefit due to the DST implementation in the presence of plant-model mismatch. The tracking ability of the multi-rate MHE is also analyzed. Finally, the computational performance of the DST is discussed.

The EAF heat considered here is of duration 60 minutes with 2 scrap charges. The economics based optimization for the plant gives an objective function value of 100 (normalized \$profit/batch). The value is represented as the *theoretical* best in Table 1. The optimization is then conducted for the model with perfect initial state knowledge and the solution is implemented on the plant to obtain an objective function value of 95.39. The *nominal* solution of 95.39 is expected because less percentage of arc power is used, in melting the scrap charge, due to the plant-model mismatch. To carry out the analysis for DST, the measurement values are corrupted with Gaussian zero mean noise.
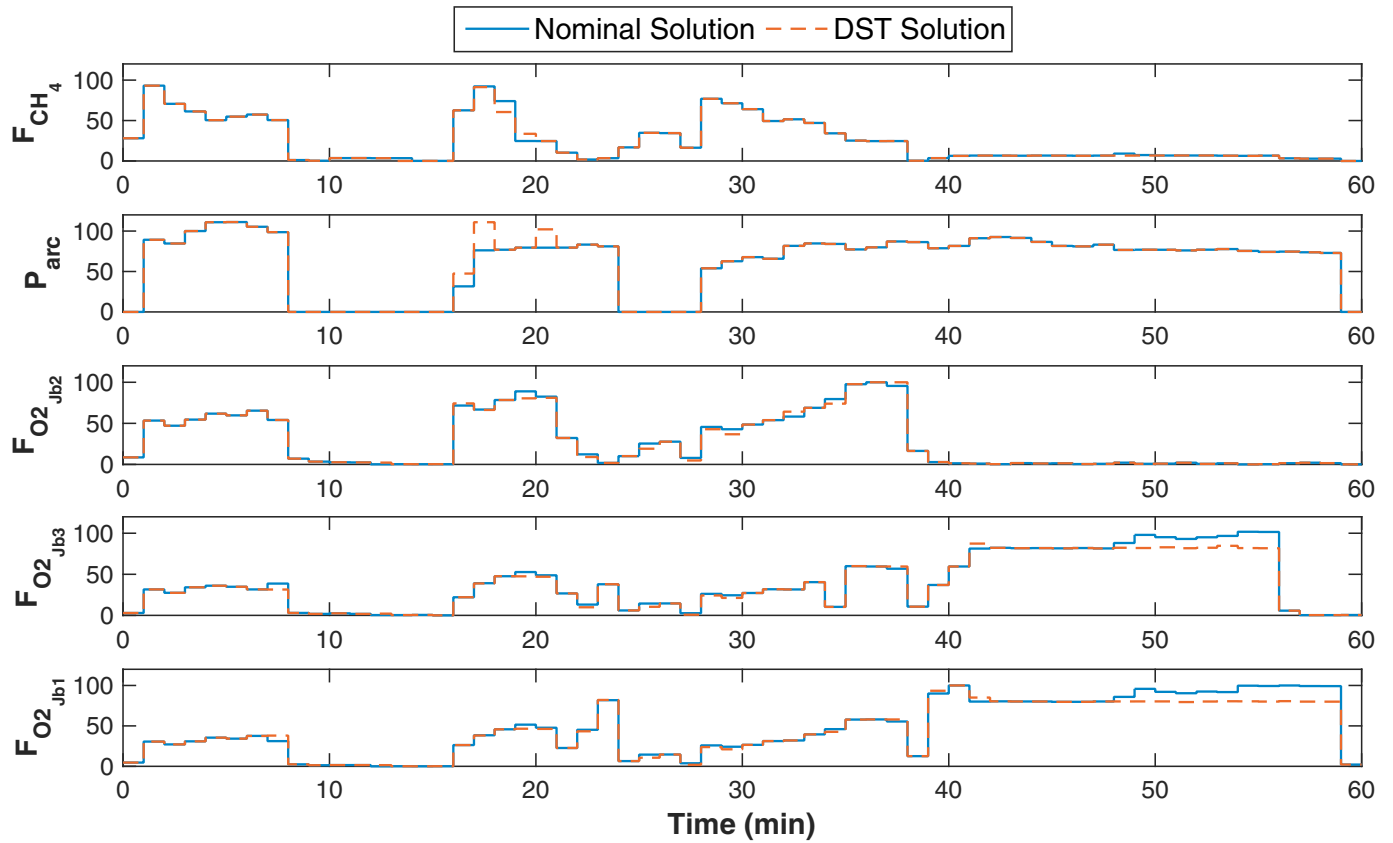
Fig. 4. Case Study: DST input profiles compared to nominal inputs.

Table 2. Measurements for the case study.

Measurement	Sampling Time	Variance
Off-gas compositions (CO, CO_2, O_2, H_2)	Every 1 min	0.01
T_{roof}, T_{wall}	Every 1 min	3
Slag compositions (FeO, Al_2O_3, SiO_2, MgO, CaO)	43rd min	0.1
Molten-metal temperature	43rd & 47th min	5
Molten-metal carbon content	43rd & 47th min	0.01

Table 3. Multi-rate measurement structure for the case study.

Time (min)	0…42	43	44…46	47	48…60
Number of measured variables	6	**13**	6	**8**	6

The measurements considered for the estimation and their corresponding variance values are given in Table 2. Table 3 shows the number of measured variables at different sampling times. Observability of the system is analyzed by checking the observability metric value, as defined in Ji and Rawlings (2015), at every time step. The system is found to be full observable with the lowest metric value as 7.0×10^{-07}. The multi-rate MHE is setup using perfect state knowledge and a estimation horizon of 6 minutes. The covariances S_0 and Q are determined by trial and error which involved analysis of multiple simulations. Lower and upper bounds are imposed for the states, the algebraic variables and the model noises. The estimated and true profiles for a selection of states is presented in figure 3. It is observed that the MHE is showing very good performance in estimating the true states despite the adverse effects of
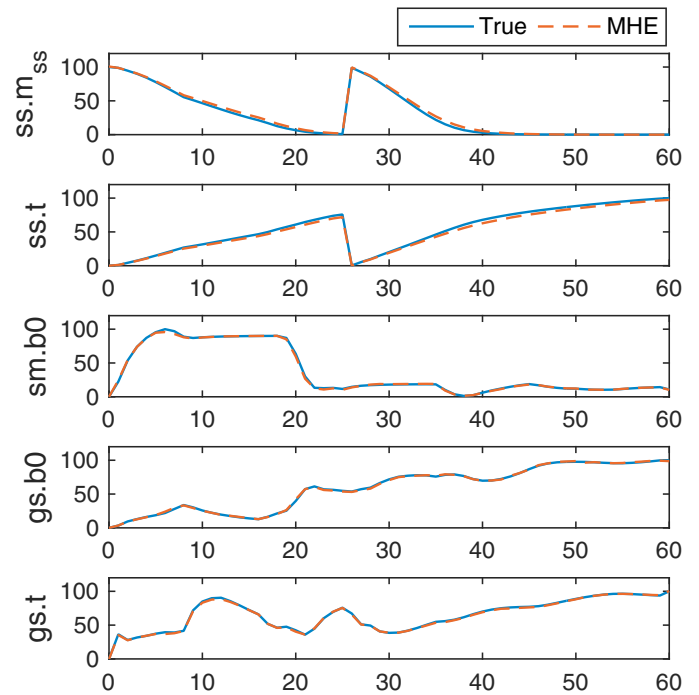

Fig. 3. State estimates with respect to time (in minutes).

plant-model mismatch and measurement noise. The strong convergence property of the MHE is reflected directly on the profit calculated using the DST. This is attributed to the fact that a state estimation procedure acts as a pathway for the plant information to flow into the model. Figure 4 shows the comparison between the DST and the nominal inputs. An objective value of 97.67 is achieved with 5 on-line re-optimizations carried out at 10th, 20th,
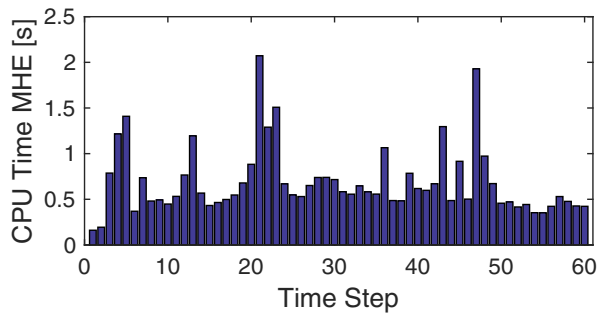
Fig. 5. Solution times for MHE problem with horizons of N = 6 time steps.

Table 4. Solution time for shrinking horizon optimization problem.

Time where DST is called by Operator (min)	10	20	30	40	50
CPU Time (s)	42.4	28.6	9.8	5.2	1.2

30th, 40th and 50th minute. The 2.4% increase in objective value due to the application of the DST would translate to a significant annual increase in profit. The economic improvement points to the need for on-line corrections and output feedback when using a first principles model for real-time applications.

4.1 Computational results

We performed the numerical computations on an Intel Core i7-3770 processor with 4 CPU cores running Windows 7 at 3.40 GHz. The solution time history (in CPU seconds) of the MHE runs is shown in figure 5. The MHE solve is very fast with a remarkably small average solve time of 0.69 s. The solution times for the shrinking horizon optimization is presented in Table 4. On average, the economic optimization problem is solved in 17.4 s. This is well below the sampling time of 1 minute.

5. CONCLUSION

In this paper, we propose an on-line DST based on multi-rate MHE for the EAF steelmaking process. The DST combines the MHE with the shrinking horizon optimizer to provide economically optimal input trajectories based on the current state of the system. The full discretization approach is used to solve the optimization problems. The proposed DST takes advantage of a detailed EAF model and can be used in real-time by EAF operators. As future work, the effect of additional sources of uncertainty will be investigated. We also intend to study the economic impact of an increase in optimizer execution frequency in the DST. Additionally, a closed-loop economic model predictive controller coupled with MHE would be a useful avenue of investigation for application for EAFs.

REFERENCES

Allgöwer, F., Badgwell, T.A., Qin, J.S., Rawlings, J.B., and Wright, S.J. (1999). Nonlinear predictive control and moving horizon estimation an introductory overview. In *Advances in Control*, 391–449. Springer.

Andersson, J. (2013). *A General-Purpose Software Framework for Dynamic Optimization*. PhD thesis, Arenberg Doctoral School, KU Leuven, Department of Electrical Engineering (ESAT/SCD) and Optimization in Engineering Center, Kasteelpark Arenberg 10, 3001-Heverlee, Belgium.

Biegler, L.T. (2007). An overview of simultaneous strategies for dynamic optimization. *Chemical Engineering and Processing: Process Intensification*, 46(11), 1043–1053.

Billings, S., Boland, F., and Nicholson, H. (1979). Electric arc furnace modelling and control. *Automatica*, 15(2), 137–148.

Ghobara, Y. (2013). *Modeling, Optimization and Estimation in Electric Arc Furnace (EAF) Operation*. Master's thesis, McMaster University.

Hindmarsh, A.C., Brown, P.N., Grant, K.E., Lee, S.L., Serban, R., Shumaker, D.E., and Woodward, C.S. (2005). SUNDIALS: Suite of nonlinear and differential/algebraic equation solvers. *ACM Transactions on Mathematical Software (TOMS)*, 31(3), 363–396.

Ji, L. and Rawlings, J.B. (2015). Application of MHE to large-scale nonlinear processes with delayed lab measurements. *Computers & Chemical Engineering*, 80, 63–72.

MacRosty, R.D.M. and Swartz, C.L.E. (2005). Dynamic modeling of an industrial electric arc furnace. *Ind.Eng.Chem.Res.*, 44, 8067–8083.

MacRosty, R.D.M. and Swartz, C.L.E. (2007). Dynamic optimization of electric arc furnace operation. *AIChE Journal*, 53, 640–653.

Matson, S. and Ramirez, W.F. (1999). Optimal operation of an electric arc furnace. In *57 th Electric Furnace Conference*, 719–730.

Oosthuizen, D., Craig, I., and Pistorius, P. (1999). Model predictive control of an electric arc furnace off-gas procedure combined with temperature control. In *Africon, 1999 IEEE*, volume 1, 415–420. IEEE.

Process Systems Enterprise Ltd. (2015). gPROMS, www.psenterprise.com/gproms, 1997-2015.

Rao, C.V., Rawlings, J.B., and Mayne, D.Q. (2003). Constrained state estimation for nonlinear discrete-time systems: Stability and moving horizon approximations. *IEEE Transactions on Automatic Control*, 48(2), 246–258.

Shyamal, S. and Swartz, C.L.E. (2016a). Multi-rate moving horizon estimation for an electric arc furnace steelmaking process. *AIChE Annual Meeting*.

Shyamal, S. and Swartz, C.L.E. (2016b). A multi-rate moving horizon estimation framework for electric arc furnace operation. *IFAC-PapersOnLine*, 49(7), 1175–1180.

Wächter, A. and Biegler, L.T. (2006). On the implementation of an interior-point filter line-search algorithm for large-scale nonlinear programming. *Mathematical Programming*, 106(1), 25–57.

Woodside, C., Pagurek, B., Pauksens, J., and Ogale, A. (1970). Singular arcs occurring in optimal electric steel refining. *IEEE Transactions on Automatic Control*, 15(5), 549–556.